

Sliding Mode Control For PV-Wind Hybrid System Connected to Grid

Houda LAABIDI^{#1}, Houda JOUINI^{*2}, Abdelkader MAMI^{*3}

[#]ESPRIT School of Engineering, Tunis, Tunisia.

^{*}University Tunis El Manar, Laboratory LAPER, Tunis, Tunisia

¹Houda.abidi@esprit.tn

²houda.jouini@gmail.com

³Abdelkader.mami@gmail.com

Abstract— This work focuses on the development of a nonlinear Sliding Mode Controller (SMC) for photovoltaic-wind hybrid energy system connected to electrical grid. Several benefits are offered by this method such as robustness against a parameter variations, minimum output current distortion and excellent reference tracking. The maximum power extracted from wind turbine and PV array is fed to utility grid via a three phase inverter interface by maintaining constant DC-link voltage. Simulation results under Psim environment show a fast dynamic behavior of hybrid system with minimal errors, accuracy and usefulness of the considered control strategy.

Keywords—SMC; hybrid system; MPPT; grid; Wind/PV

I. INTRODUCTION

Applications with ecological and renewable resources such as wind and photovoltaic energies have become the major promising technologies. They have been improved significantly in the last decades due to the high petroleum prices, the harmful effects caused by conventional sources on the planet and increasing energy demand [1]. Particularly, photovoltaic and wind generation systems have enhanced their employment in hybrid configurations. The considered combination is one of the most efficient key used as a grid-connected energy systems or an isolated load to supply power. At present, many investigations have been carried out on the PV-Wind hybrid system techniques. The most traditionally strategies based on linear controllers were presented by (Bariša et al, 2015),[2] showing that the Field Oriented Control (FOC) is separately controls the electromagnetic torque and the magnetic flux. Another study given by [3], have focused on power Voltage Oriented Control (VOC) due to its simple structures. One of the most remarkable drawbacks is their highly dependence on machine parameter variations. Another control techniques mentioned by some authors are based on non-linear hysteresis control such as Direct Power Control (DPC) [4] and Direct Torque Control (DTC)[5]. The switching frequency variation is the main drawbacks of these methods which cause the grid current distortions.

In this context, this paper aims to analyse a connected grid hybrid system behavior under different climatic conditions. This study is organized as follows; the PV-Wind system structure and its components modeling are introduced in the first section. Then MPPT method and Sliding Mode Controller (SMC) design for back to back converter are detailed. Simulation results and discussions are presented in the last section in order to evaluate the proposed photovoltaic -wind system configuration performances.

II. PV-WIND SYSTEM CONFIGURATION

The proposed PV-Wind hybrid power system is described by Fig 1. it is composed of two parallel conversion chains. The first one consists of the photovoltaic power system which includes a PV module as energy source and DC/DC converter using a boost chopper. The wind energy conversion system presents the second chain that is equipped with its variable speed wind turbine coupled to Permanent Magnet Synchronous Generator (PMSG) and a three phase rectifier. The hybrid system is connected to grid via DC/AC inverter linked to RL filter to eliminate the current harmonics. The mathematical models of each block are introduced in the following subsections.

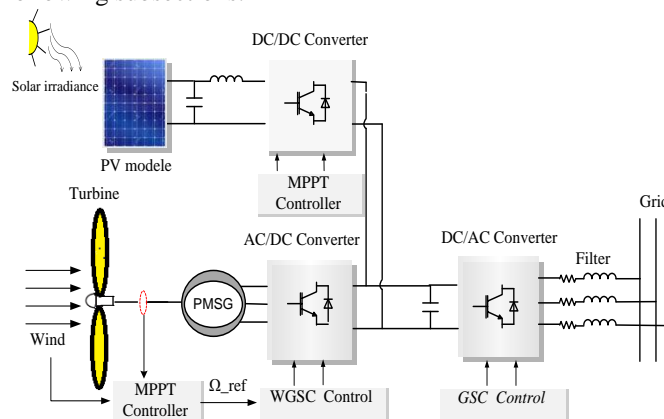


Fig.1: Photovoltaic-wind hybrid system

A. Photovoltaic chain modeling

The photovoltaic cells are characterized by the non-linear curves. These curves are determined the most important

These curves are determined by the important parameters given by the cell manufacturer. The maximum power point is the nominal operating point for which the PV module can deliver the maximum power. P&O and Incremental Conductance (INC) algorithms are the most commonly used MPPT methods [6]; P&O algorithm is widely used due to its easy implementation. However Incremental Conductance (INC) strategy can precisely track the maximum power point, with a faster dynamic response under rapidly weather conditions changing. Thus, Fig.2 shows MPPT controller based on Incremental Conductance (Inc.Cond) algorithm which is used in the PV system to force the DC/DC converter circuit to track the maximum power for different solar irradiances.

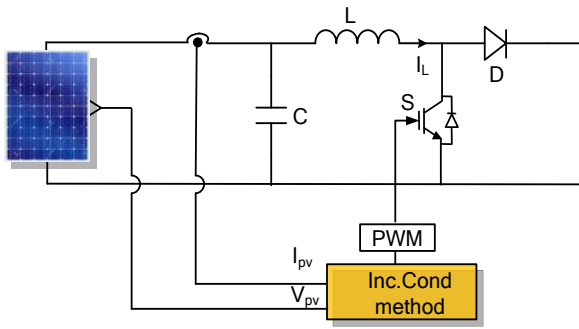


Fig.2 : Photovoltaic module characteristics

B. Wind energy chain modeling

1) Wind turbine model

The mechanical power produced by the wind turbine can be calculated by the following equation :

$$P_t = \frac{1}{2} \cdot \rho \cdot \pi \cdot R_t^2 C_p(\lambda, \beta) V_w^3 \quad (1)$$

Where ρ is the air specific density (kg/m³), R_t is the wind turbine rotor radius (m), V_w is the wind speed (m/s), $C_p(\lambda, \beta)$ is the turbine power coefficient, β is the blade pitch angle and λ is the tip-speed ratio which is expressed as [7]:

$$\lambda = \frac{\Omega_r \cdot R_t}{V_w} \quad (2)$$

where Ω_r is the rotor angular speed (rad/s). Many power coefficient approximations are mentioned in literature; among these forms we choose this expression.

$$C_p(\lambda, \beta) = c_1 \left(\frac{c_2}{\lambda_i} - c_3 \cdot \beta - c_4 \right) \cdot e^{-\frac{c_5}{\lambda_i}} + c_6 \cdot \lambda \quad (3)$$

with

$$\frac{1}{\lambda_i} = \frac{1}{\lambda + 0.08 \cdot \beta} - \frac{0.035}{\beta^3 + 1} \quad (4)$$

The coefficients are: $c_1 = 0.5176$, $c_2 = 116$, $c_3 = 0.3$, $c_4 = 5$, $c_5 = 21$ and $c_6 = 0.0068$.

The mechanical torque (T_m) expression can be developed as given in the Equation (5).

$$T_m = \frac{P_t}{\Omega_r} = C_p \cdot \frac{\rho \cdot S \cdot V_w^3}{2} \cdot \frac{1}{\Omega_r} \quad (5)$$

2) Permanent Magnet Synchronous Generator (PMSG)

The electrical model of the PMSG in a (d, q) reference frame, is written by the following equations [8]

$$\begin{cases} \frac{di_{ds}}{dt} = -\frac{R_s}{L_d} \cdot i_{ds} + \frac{\omega_r \cdot L_q}{L_d} \cdot i_{qs} + \frac{V_{ds}}{L_d} \\ \frac{di_{qs}}{dt} = -\frac{R_s}{L_q} \cdot i_{qs} - \frac{\omega_r \cdot L_d}{L_q} \cdot i_{ds} - \frac{\omega_r \cdot \phi_f}{L_q} + \frac{V_{qs}}{L_q} \\ \frac{d\Omega_r}{dt} = \frac{C_m}{J} - \frac{T_{em}}{J} - \frac{f}{J} \cdot \Omega_r \end{cases} \quad (6)$$

where V_{ds} and V_{qs} are, respectively, the d-axis and q-axis stator voltage (V), i_{ds} , i_{qs} are the d-axis and q-axis stator current(A), R_s is the resistance of stator windings (Ω), L_d , L_q are the inductance of stator windings (mH), ϕ_f is the permanent magnetic flux (wb), ω_r electrical pulsation (rad/s) and p is the number of pole pairs of the PMSG.

The active and reactive powers are given by :

$$\begin{cases} P = \frac{3}{2} (V_{ds} \cdot i_{ds} + V_{qs} \cdot i_{qs}) \\ Q = \frac{3}{2} (V_{qs} \cdot i_{ds} - V_{ds} \cdot i_{qs}) \end{cases} \quad (7)$$

The mechanical equation is expressed as follows:

$$T_m - T_{em} = J_t \cdot \frac{d\Omega_r}{dt} + f \cdot \Omega_r \quad (8)$$

The PMSG electromagnetic torque can be expressed using the following equation:

$$T_{em} = \frac{3}{2} \cdot p \cdot \phi_f \cdot i_{qs} \quad (9)$$

In order to deliver the entire electrical power to the grid, a back-to-back converter are controlled using the sliding mode strategy. For that, two sliding mode are required and detailed in the next section: one to the AC/DC Rectifier and one to the DC/AC inverter.

III. SLIDING MODE CONTROLLER METHOD

The sliding mode controller design is mainly involved three steps. The appropriate sliding mode surfaces choice is done in the first step. The general equation used to choose these sliding surfaces is proposed by [9] [10]:

$$S(X) = \left(\frac{d}{dt} + \lambda\right)^{r-1} (X^d - X) \quad (10)$$

Where: X: state variable of the control signal; λ : positive constant; r: the system degree; X^d : the desired signal.

In order to ensure the convergence towards the sliding surface trajectory; the convergence condition based on Lyapunov equation is defined in the second step .

$$S(X)S(\dot{X}) < 0 \quad (11)$$

Finally, the control signal calculation is expressed by the following relation:

$$U = U_{eq} + U_n \quad (12)$$

where U_{eq} is the equivalent control and U_n is the switching control term.

A. SMC For AC/DC Rectifier

The three phase rectifier used in the wind energy conversion chain is controlled by a sliding mode method in order to obtain the maximum wind power according to variable weather conditions. To achieve these objectives; two control loops are presented in Fig 3; external speed control loop and inner current control loop. Among the different used modern strategies, SMC is intended for non-linear systems since it has robust characteristics against uncertain system parameter and external disturbances.

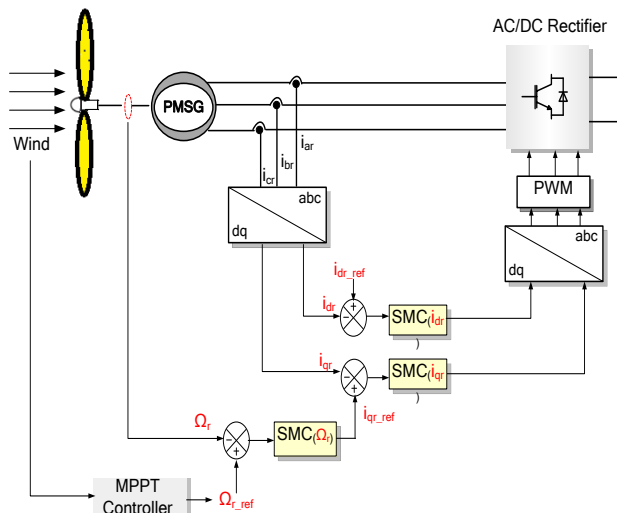


Fig 3. Generator Side Converter Control

1) External speed control loop

the surface $S(\Omega_r)$ is chosen as:

$$S(\Omega_r) = \Omega_{r_ref} - \Omega_r \quad (13)$$

Ω_{r_ref} is the reference value of generator speed

During the steady state, the surface $S(\Omega_r)$ is equal to zero as its derivative:

$$S(\dot{\Omega}_r) = \dot{\Omega}_{r_ref} - \dot{\Omega}_r \quad (14)$$

$$S(\dot{\Omega}_r) = -\frac{C_m}{J} + \frac{C_{em}}{J} + \frac{f}{J}\Omega_r \quad (15)$$

So, the quadrature stator current reference is defined by:

$$i_{qs_ref} = i_{qs_eq} + i_{qs_n} \quad (16)$$

the equivalent control i_{qs_eq} is expressed as follows

$$i_{qs_eq} = \frac{2}{3} \cdot \frac{J \cdot \dot{\Omega}_{r_ref} - C_m - f \cdot \Omega_r}{p \cdot (\phi_r + (L_q - L_d) \cdot i_{ds})} \quad (17)$$

the switching control is written as:

$$i_{qs_n} = -K_{\Omega} \cdot \text{sign}(S(\Omega_r)), \quad (18)$$

2) Inner current control loop

Two sliding surfaces are required to control d- and q- axis stator current components :

$$\begin{cases} S(i_{ds}) = i_{ds_ref} - i_{ds} \\ S(i_{qs}) = i_{qs_ref} - i_{qs} \end{cases} \quad (19)$$

where i_{ds_ref} and i_{qs_ref} are the stator current references,

The sliding surfaces and their derivatives should validate the following conditions :

$$S(i_{ds})S(\dot{i}_{ds}) < 0$$

$$S(i_{qs})S(\dot{i}_{qs}) < 0 \quad (20)$$

The derivative of these surfaces are given by:

$$\begin{cases} S(\dot{i}_{ds}) = \frac{R_s}{L_d} \cdot i_{ds} - \frac{p \cdot \Omega_r \cdot L_q}{L_d} \cdot i_{qs} - \frac{V_{ds}}{L_d} \\ S(\dot{i}_{qs}) = \frac{R_s}{L_q} \cdot i_{qs} + \frac{p \cdot \Omega_r \cdot L_d}{L_q} \cdot i_{ds} + \frac{p \cdot \Omega_r \cdot \phi_r}{L_q} - \frac{V_{qs}}{L_q} \end{cases} \quad (21)$$

Therefore ,the d-axis controlled voltage is defined by the continuous and the discontinuous components voltage:

$$V_{ds_ref} = V_{ds_eq} + V_{ds_n} \quad (22)$$

During the steady state, the surface $S(i_{ds})$ is equal to zero, as well as its derivative, which leads to the expression of the equivalent command V_{ds_eq} is given by :

$$V_{ds_eq} = R_s \cdot i_{ds} - p \cdot \Omega_r \cdot L_q \cdot i_{qs} \quad (23)$$

and

$$V_{ds_n} = K_{ds} \cdot \text{sign}(S(i_{ds})); K_{ds} > 0 \quad (24)$$

the d-axis controlled voltage is defined by:

$$V_{qs_ref} = V_{qs_eq} + V_{qs_n} \quad (25)$$

Where

$$V_{qs_eq} = R_s \cdot i_{qs} - p \cdot \Omega_r \cdot L_q \cdot i_{ds} + p \cdot \Omega_r \cdot \phi_f \quad (26)$$

and

$$V_{qs_n} = K_{qs} \cdot \text{sign}(S(i_{ds})); K_{qs} > 0 \quad (27)$$

B. SMC For DC/AC Inverter

The proposed control scheme of the grid connected inverter consists of three parts Fig. 4. Adjusting the DC-link voltage is the first part which is usually focused on the DC-link voltage control (V_{dc}) by using PI regulator in order to generate the reference value of d-axis current. the second one is intended to regulate the grid currents by using sliding mode controller (SMC). The grid synchronisation method is the last part adopted to synchronize between the grid-interfacing inverter and the electrical grid. It is based on PLL(Phase Locked Loop) technique.

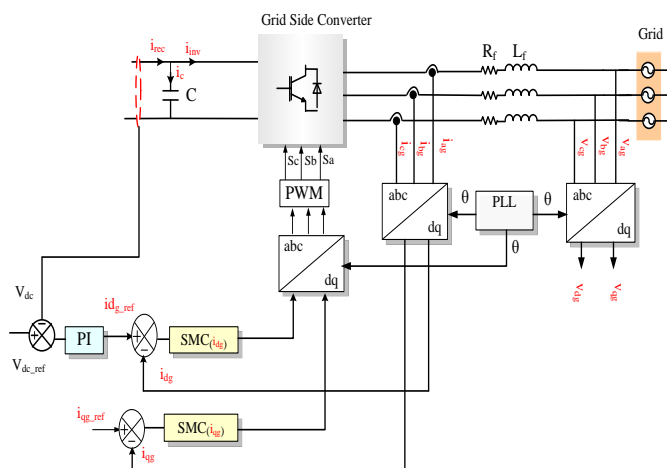


Fig.4: Grid Side Converter Control

1) DC link voltage loop

The external DC-link voltage loop is based on PI controller;

the DC bus voltage V_{dc} is written as:

$$V_{dc} = \frac{1}{C \cdot p} i_c = \frac{1}{C \cdot p} (i_{rec} - i_{inv}) \quad (28)$$

The transfer current of DC-link voltage control loop is expressed as:

$$\frac{V_{dc}}{V_{dc_ref}} = \frac{\frac{k_p}{C} p + \frac{k_i}{C}}{p^2 + \frac{k_p}{C} p + \frac{k_i}{C}} \quad (29)$$

The PI controller parameters k_p and k_i are tuned as follows by imposing the natural oscillations frequency ω_n and damping ratio ξ values.

$$\begin{cases} k_p = 2C\xi\omega_n \\ k_i = C\omega_n^2 \end{cases} \quad (30)$$

2) DC link voltage loop

Two switching surfaces are chosen $S(i_{dg})$ and $S(i_{qg})$ in order to regulate d-axis and q-axis grid current components .

$$\begin{cases} S(i_{dg}) = i_{dg_ref} - i_{dg} \\ S(i_{qg}) = i_{qg_ref} - i_{qg} \end{cases} \quad (31)$$

Where i_{dg} , i_{qg} are the desired current values of d and q axis; The current references i_{dg_ref} and i_{qg_ref} are maintained constants. Therefore , the sliding surfaces derivatives can be written as follows:

$$\begin{cases} S(i_{dg}) = i_{dg_ref} - i_{dg} = -\dot{i}_{dg} = \frac{1}{L_f}(v_{dg} + R_f i_{dg} - \omega_f L_f i_{qg} - e_{dg}) \\ S(i_{qg}) = i_{qg_ref} - i_{qg} = -\dot{i}_{qg} = \frac{1}{L_f}(R_f i_{qg} + \omega_f L_f i_{dg} - e_{qg}) \end{cases} \quad (32)$$

The sliding surfaces and their derivatives should validate the following conditions :

$$\begin{cases} S(i_{dg})S(\dot{i}_{dg}) < 0 \\ S(i_{qg})S(\dot{i}_{qg}) < 0 \end{cases} \quad (33)$$

Therefore ,the d-axis controlled voltage is defined by:

$$v_{dg_ref} = v_{dg_eq} + v_{dg_n} \quad (34)$$

with

$$\begin{cases} v_{dg_eq} = v_{dg} + R_f i_{dg} - \omega_f L_f i_{qg} \\ v_{dg_n} = k_{dg} \text{sgn}S(i_{dg}); k_{dg} > 0 \end{cases} \quad (35)$$

the q-axis controlled voltage is defined by

$$v_{qg_ref} = v_{qg_eq} + v_{qg_n} \quad (36)$$

with

$$\begin{cases} v_{qg_{eq}} = R_f i_{qg} + \omega_f L_f i_{dg} \\ v_{qg_n} = k_{qg} \operatorname{sgn}S(i_{qg}); q > 0 \end{cases} \quad (37)$$

IV. SIMULATION RESULTS

As a perspective to test the effectiveness of the proposed sliding mode controller to the PV - wind hybrid system, many Simulations were carried out using PSIM Software using the system parameters listed in table I.

TABLE I: Parameters of PV module and wind Turbine

PARAMETER	Value
Maximum Power Point [Pmpp]	200W
Maximum Power Point Voltage [Vmpp]	26.3V
Maximum Power Point Current [Impp]	7.61A
Open Circuit Voltage [Voc]	32.9V
Short Circuit Current [Isc]	8.21A
Rated turbine Power	19 KW
Rated Wind Speed	10m/s
Air Density	1.22 kg/m ³

Case 1: The Photovoltaic system response

The proposed photovoltaic system configuration consists of 36 PV modules distributed as ten modules in series and three arrangements in parallel. The simulation of this photovoltaic chain performances is based on solar condition level variations when the temperature T is kept constant at 25°C as shown in Fig.5. At t=1 sec irradiation level is increased from 700 to 1000 W/m² and decreased from 1000 W/m² to 400 W/m² at t=2sec. Fig.5 (b-c-d) illustrates ,respectively, the output PV power, current and voltage behaviors when facing the solar irradiation changes. It can be seen that the PV array is able to deliver a maximum power of 18.8 kW at 1000W/m². The power generated using Inc.Cond MPPT Controller is followed the optimal power with a good accuracy. It can be shown also that the V_{pv} array voltage is about 460 V. However the maximum output current I_{pv} is highly dependent on solar irradiance variation.

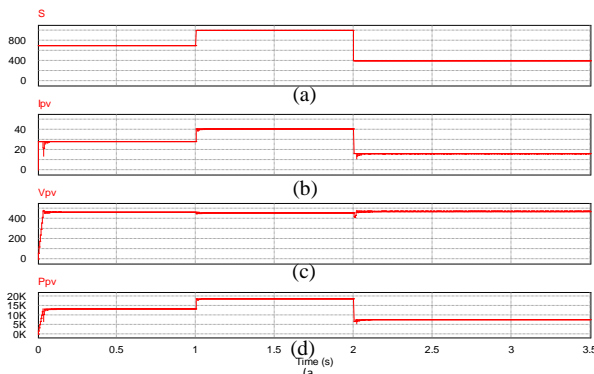


Fig.5 PV system performances under varying solar irradiance

Case 2: The Wind system response

The wind speed is dropped from 10 m/s to 6m/s at t=1.5sec and is increased from 6 m/s to 8 m/s at t=2.5s as shown in Fig.6 (a). An excellent PMSG rotor speed tracking to the reference speed is depicted in Fig.6 (b). The rotational speed Omega_r is well monitored and controlled according to the captured wind velocity with a rapid dynamic performance. It is illustrated also that the generator torque Tm can follow proportionally the abrupt wind speed variations as shown in Fig.6 (c). The MPPT block is able to calculate the actual optimal rotation speed and generate the maximum power P_turbine equal to 18.5kW shown in Fig. 6.

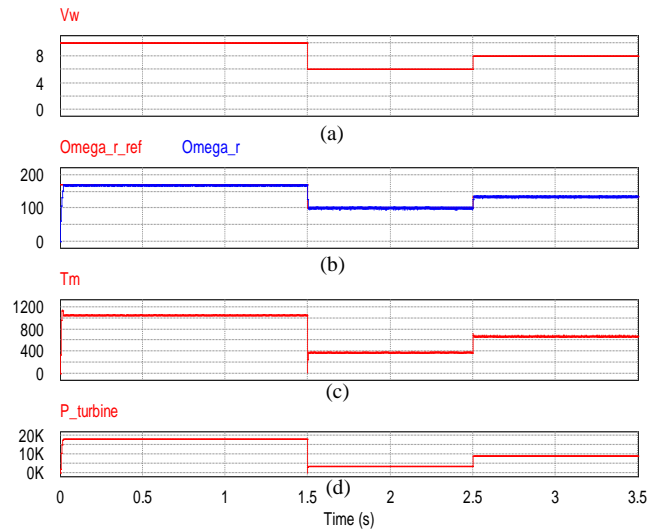


Fig.6 : Wind system performances under wind speed variations

Case 3: The grid side inverter response

The PV array and the wind turbine sources provide together the active power (P_active ≈37.3 kW) injected by three phase inverter into the grid as shown in Fig.7. It is clear that the active power is highly related to the different solar irradiance and wind speed profile variations. However the delivered reactive power (Q_reactive) is fixed at zero to keep the unity power factor . The DC-link voltage is maintained constant at 700 V over the time period of 3.5 sec; it follows correctly its reference value (Fig.8). The injected current (i_ag) should be in phase with the grid voltage (v_ag) proving unity power factor transmission as shown in Fig.9 and finally the grid currents have a sinusoidal waveforms with a constant grid frequency value equal to 50 Hz thereby confirming the usefulness of the established SMC controller (Fig.10).

The simulation results reveal that the developed SMC method under divers operating weather conditions present an excellent dynamic response and very good steady state performances .

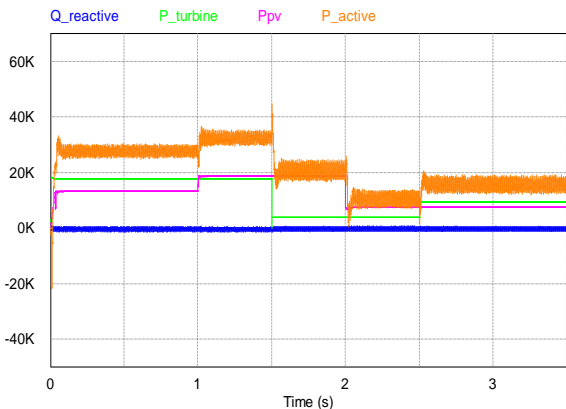


Fig. 7. PV-Wind system performances under different solar irradiance and Wind speed levels

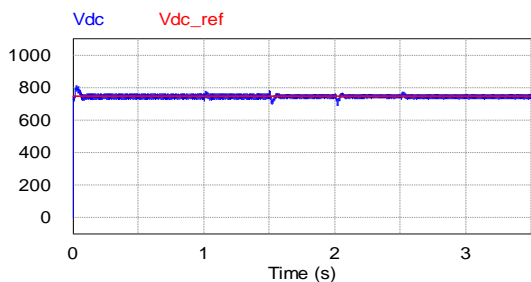


Fig.8.PV-Wind system performances under different solar irradiance and Wind speed levels

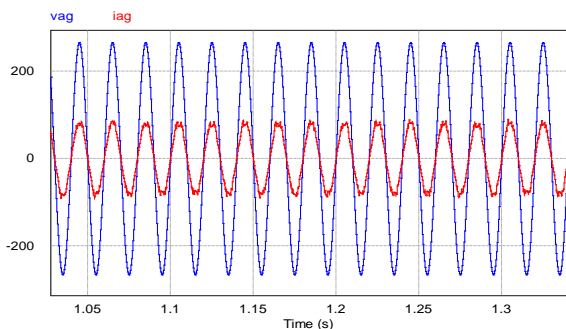


Fig.9. Current and voltage grid

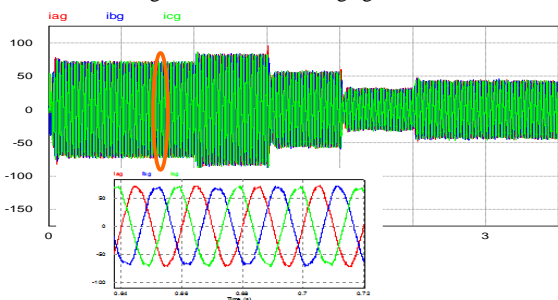


Fig.10. Grid current waveforms

IV. CONCLUSION

The proposed hybrid system has been tested using sliding mode controller for different weather cases by evaluating the following performances; the maximum power is extracted from renewable energy sources, the DC-link voltage is maintained at constant level, the reactive power injected to the grid is set at zero in order to achieve the unity power factor condition. All results shown, verify the usefulness of the proposed PV-Wind hybrid system techniques.

References

- [1] Jin Yi, Xinyu Lt, Liang Gao, Yongping Chen, Optimal Design of Photovoltaic-Wind Hybrid Renewable Energy System using a Discrete Geometric Selective Harmony Search, 2015 IEEE 19th International Conference on Computer Supported Cooperative Work in Design (CSCWD), September 2015.
- [2] T.Barisa, D.Sumina, M.Kutija, Control of generator- and grid-side converter for the interior permanent magnet synchronous generator, International Conference on Renewable Energy Research and Applications, February 2016.
- [3] Y. Errami, M. Ouassaid, M. Maaroufi, Modelling and optimal power control for permanent magnet synchronous generator wind turbine system connected to utility grid with fault conditions, World Journal of Modelling and Simulation, Vol. 11 (2015) No. 2, pp. 123-135.
- [4] F.louar, A.ouari, A.omeiri, F.senani, A.Rahab, Direct power control (DPC) of PMSG based wind energy conversion system, 4th International Conference on Electrical Engineering (ICEE), February 2016.
- [5] Z. Zhang; R. Kennel; C. Hackl, two direct torque and power control methods for back-to-back power converter PMSG wind turbine systems, 8th International Power Electronics and Motion Control Conference (IPEMC-ECCE Asia),2016.
- [6] Pratik U. Mankar and R.M. Moharil, comparative analysis of the perturb and observe and incremental conductance MPPT methods, International Journal of Research in Engineering and Applied Sciences, July 2014.
- [7] Vijayalakshmi S,Saikumar .S, Saravanan.S, Sandip .R.V,Sridhar Vijay, Modelling and control of a Wind Turbine using Permanent Magnet Synchronous Generator, International Journal of Engineering Science and Technology (IJEST), (2011), Vol. 3 No. 3.
- [8] Y. Errami, M.Hilal, M. Ouassaid, Variable Structure Control Approach for Grid Connected PMSG Wind Farm. International Renewable and Sustainable Energy Conference (IRSEC), 2014.
- [9] M. Nasiri, J. Milimonfared and S. H. Fathi, Robust Control of PMSG-based Wind Turbine under Grid Fault Conditions, Indian Journal of Science and Technology, Vol 8(13), 52201, July 2015.
- [10] R. Benadli; A. Sellami, Sliding mode control of a photovoltaic-wind hybrid system, International Conference on Electrical Sciences and Technologies in Maghreb (CISTEM), November 2014.